Electronic Supplementary Material (ESI) for Journal of Materials Chemistry A.

Supporting Information for

A robust multifunctional metal-organic polyhedra for high proton conductivity and selective CO_2-capture

Wen-Hao Xing,[a] Hai-Yang Li,[a] Xi-Yan Dong,*[ab] and Shuang-Quan Zang*[a]

[a] College of Chemistry and Molecular Engineering, Zhengzhou University,

Zhengzhou 450001, China.

[b] College of Chemistry and Chemical Engineering, Henan Polytechnic University,

Jiaozuo 454000, China.

*E-mail: dongxiyan0720@hpu.edu.cn (X-Y Dong); zangsqzg@zzu.edu.cn (S-Q Zang)

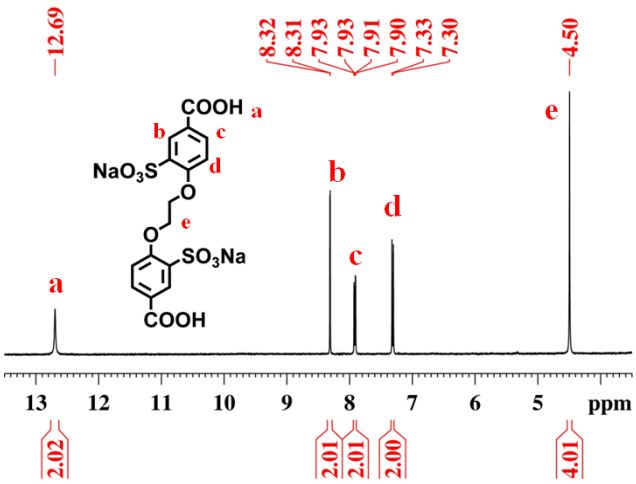

Figure S1 NMR Spectra of Na_2H_2L

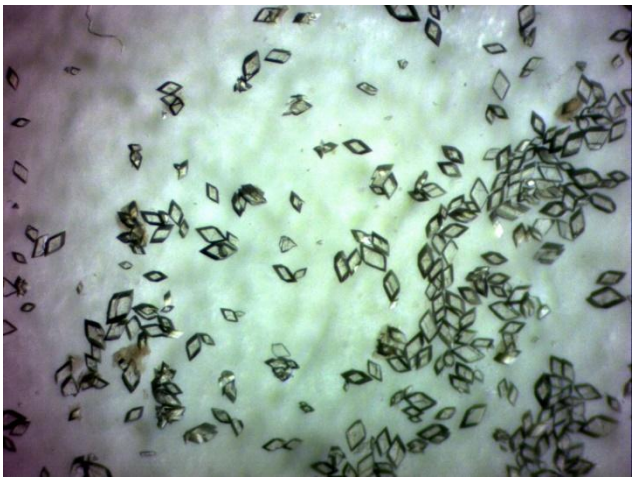

Figure S2. Optical image of MOP-1

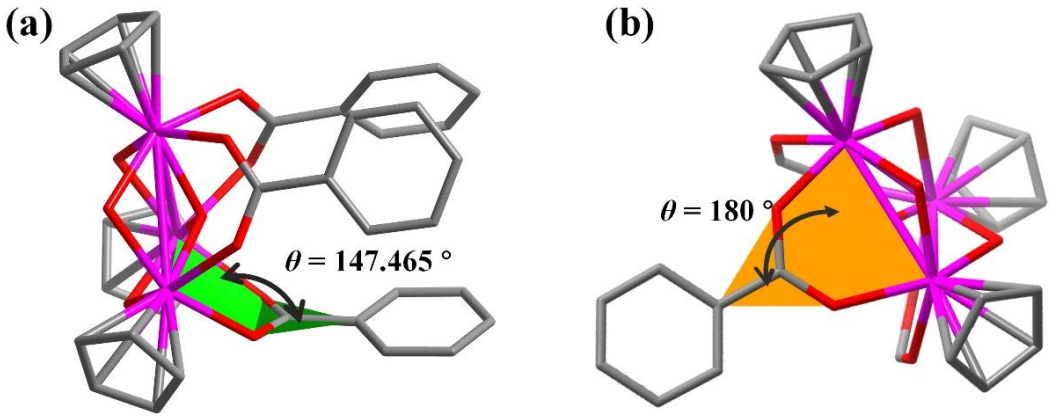

Figure S3. The included angle between the plane determined by zirconium and carboxylate and the plane determined by ligand in MOP-1(a) and in previous work (b).[1]

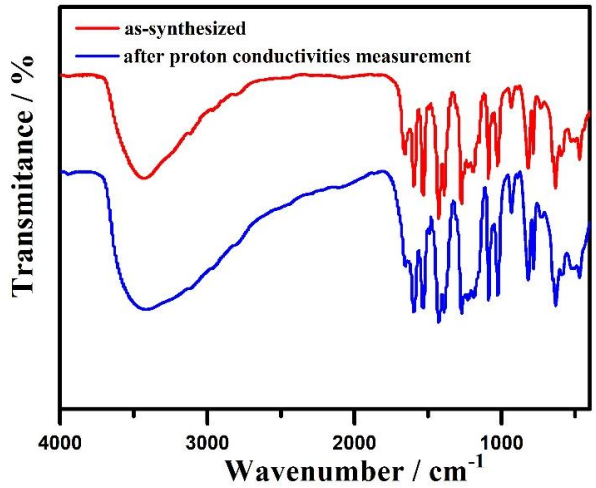

Figure S4. ATR-IR spectrum of MOP-1.

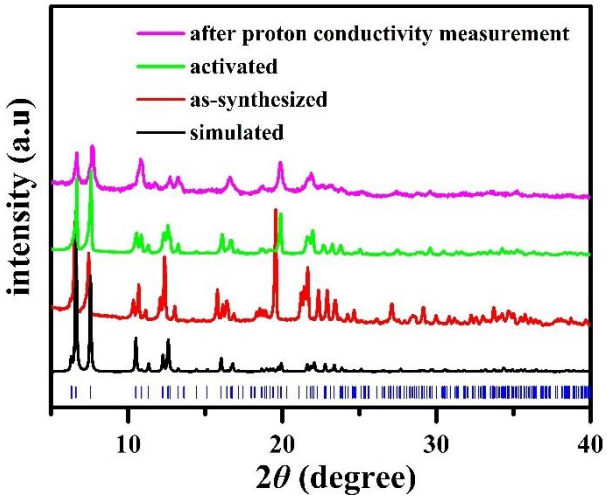

Figure S5. PXRD patterns of the samples of MOP-1 after proton conductivity measurement (magenta), the activated (green), the as-synthesized sample (red), and the simulated PXRD (black).

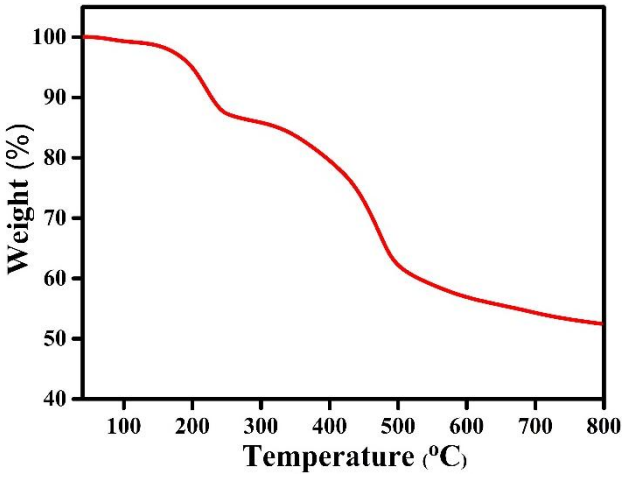

Figure S6. Thermal gravimetric curves for MOP-1

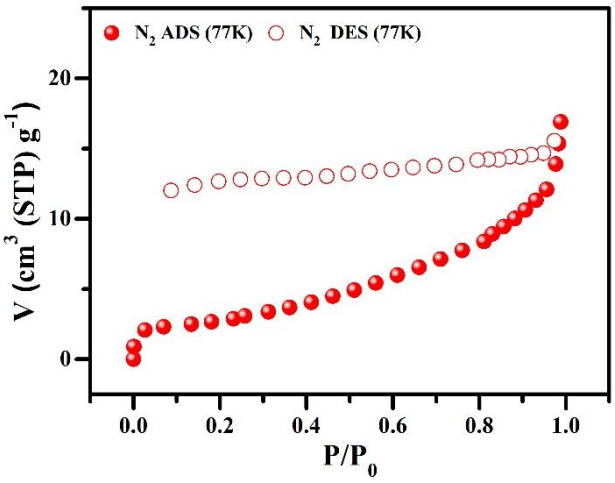

Fiure S7. N_2 sorption data at 77 K.

The IAST-predicted separation selectivity

The pure-component CO_2 and N_2 adsorption isotherm data of measured at 298 K were fitted with the dual-site Langmuir model

$$\boldsymbol{Q = Q_1 \frac{k_1 P}{1+k_1 P} + Q_2 \frac{k_2 P}{1+k_2 P}} \qquad (1)$$

where, P is the pressure of the bulk gas at equilibrium with the adsorbed phase (kPa), $\boldsymbol{Q}$ is the adsorbed amount per mass of adsorbent ($cm^3\ kg^{-1}$), $\boldsymbol{Q1}$ and $\boldsymbol{Q_2}$ are the saturation capacities of sites 1 and 2 ($cm^3\ kg^{-1}$), $\boldsymbol{k_1}$ and $\boldsymbol{k_2}$ are the affinity coefficients of sites 1 and 2 (kPa^{-1}).

A DL-IAST model can be obtained by combining IAST with dual-site Langmuir model.[2, 3] When the mixture reaches equilibrium, the simplification pressure of component ***i*** and component ***j*** are equal, and can get the mole fraction of component ***i*** in the adsorption phase.

$$\boldsymbol{Q_{1i} Ln\left(1+\frac{k_{1i} Y_i P_t}{X_i}\right) - Q_{1j} Ln\left(1+\frac{k_{1j} Y_j P_t}{X_j}\right) + Q_{2i} Ln\left(1+\frac{k_{2i} Y_i P_t}{X_i}\right) - Q_{2j} Ln\left(1+\frac{k_{2j} Y_j P_t}{X_j}\right) = 0} \qquad (2)$$

$\boldsymbol{Q_{1i}}$, $\boldsymbol{k_{1i}}$, $\boldsymbol{Q_{2i}}$ and $\boldsymbol{k_{2i}}$ are the DL model parameters of component ***i***. $\boldsymbol{Q_{1j}}$, $\boldsymbol{k_{1j}}$, $\boldsymbol{Q_{2j}}$ and $\boldsymbol{k_{2j}}$ are the DL model parameters of component ***j***, and $\boldsymbol{Y_i}$ is the mole fraction of component ***i*** in the gas phase, $\boldsymbol{X_i}$ is the mole fraction of component ***i*** in the adsorption phase. For a given $\boldsymbol{P_t}$ (equilibrium pressure) and $\boldsymbol{Y_i}$, $\boldsymbol{X_i}$ can be solved by the nonlinear numerical equation in MATLAB.

The selectivity of preferential adsorption of component ***i*** over component ***j*** in a mixture containing ***i*** and ***j***, perhaps in the presence of other components too, can be formally defined as

$$\boldsymbol{S = \frac{X_i / Y_i}{X_j / Y_j}} \qquad (3)$$

where, X_i and X_j are the mole fractions of component ***i*** and component ***j*** in the adsorption phase; Y_i and Y_j are components ***i*** and ***j*** in the gas phase scores.

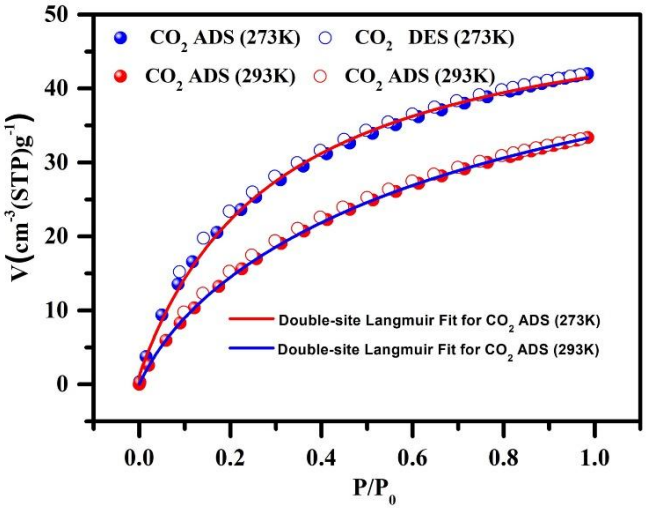

model	Double-site Langmuir		
Equiation	$Q = (Q_1*k_1*p)/(1+k_1*p)+(Q_2*k_2*p)/(1+k_2*p)$		
CO2 ADS (273K)	Reduced Chi-Sqr		0.19269
	Adj. R-Square		0.99893
		value	Standard error
	Q_1	1.20405	0.30624
	k_1	−432505.298876	3.212E6
	Q_2	52.61438	0.46128
	k_2	3.32394	0.11699
CO2 ADS (293K)	Reduced Chi-Sqr		0.00145
	Adj. R-Square		0.99999
		value	Standard error
	Q_1	8.06819	0.92405
	k_1	9.38975	0.95531
	Q_2	48.53332	0.4652
	k_2	1.17301	0.05257

Figure S8. CO_2 isotherm sorption data at 273 and 293 K for MOP-1 and nonlinear curve fitting suing Double-site Langmuir.

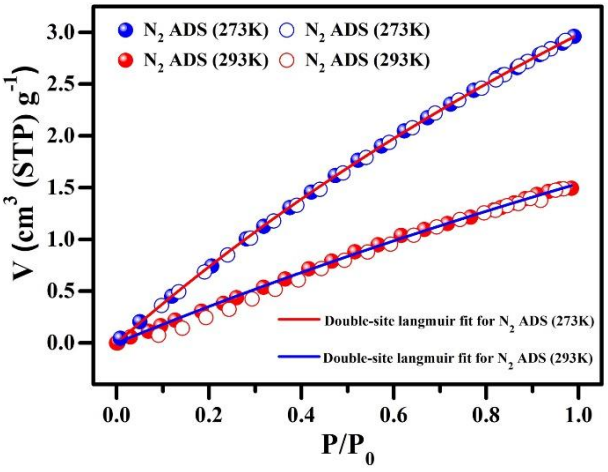

model	Double-site Langmuir		
Equiation	$Q = (Q_1*k_1*p)/(1+k_1*p)+(Q_2*k_2*p)/(1+k_2*p)$		
N_2 ADS (273K)	Reduced Chi-Sqr		4.5374E-5
	Adj. R-Square		0.99995
		value	Standard error
	Q_1	6.26316	639291.04522
	k_1	0.31206	28252.94027
	Q_2	6.26316	639291.04522
	k_2	0.31206	28252.94027
N_2 ADS (293K)	Reduced Chi-Sqr		1.94119E-4
	Adj. R-Square		0.99929
		value	Standard error
	Q_1	4.86732	9124.89856
	k_1	0.18798	0
	Q_2	4.86732	4.86732
	k_2	0.18798	0

Figure S9. N_2 isotherm sorption data at 273 and 293 K for MOP-1 and nonlinear curve fitting suing Double-site Langmuir.

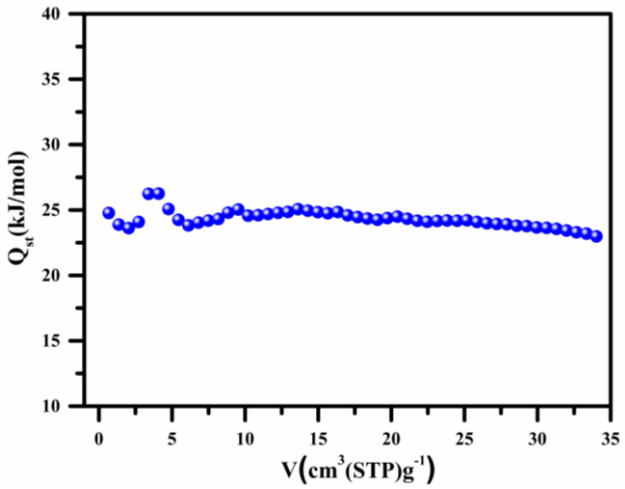

Figure S10. The CO_2 isosteric heats of adsorption (Q_{st}) of MOP-1

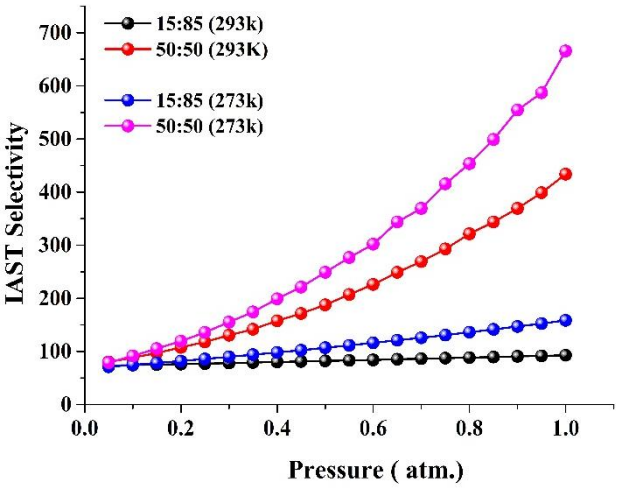

Figure S11. IAST Selectivity for MOP-1**.**

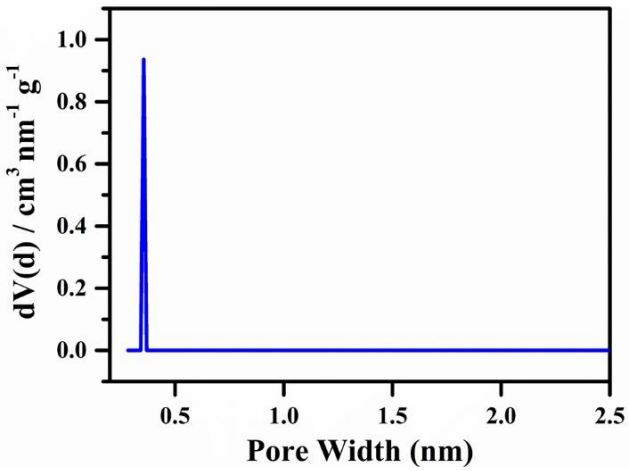

Figure S12. Pore size distribution in the range of 0.28 – 2.5 nm of MOP-1.

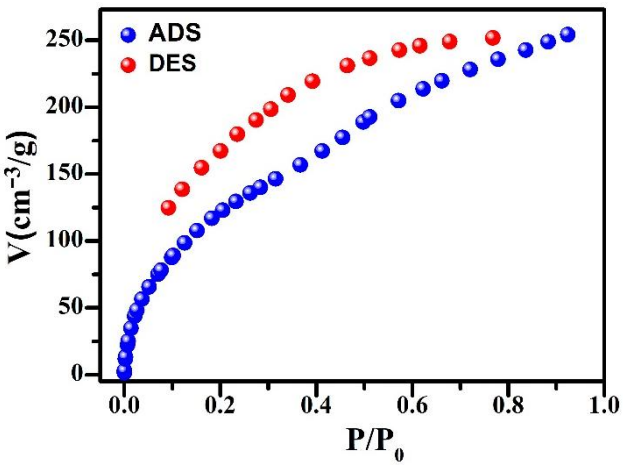

Figure S13. Water adsorption and desorption isotherms of MOP-1

The peoton conductivity studies

The conductivity (**σ**, S cm^{-1}) of the sample was obtained as follows:

$$\sigma = \frac{l}{AR} \qquad (4)$$

where **l** (cm), **A** (cm^2), and **R** (U) are the piece thickness, piece area, and resistance value, respectively. The proton transport activation energy derived from the Arrhenius equation, expressed as follows:

$$\ln(\sigma T) = \ln A - \frac{Ea}{k_B T} \qquad (5)$$

where the symbol **σ** is the proton conductivity, **Ea** represents the proton transport activation energy, $\mathbf{k_B}$ is the Boltzmann constant, and **A** is the pre-exponential factor.

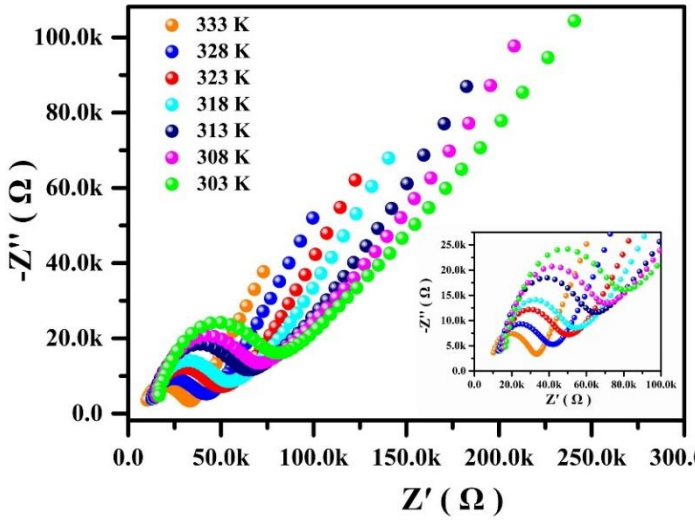

Temperature (k)	Conductivity (S cm^{-1})
303	6.28×10^{-6}
308	7.11×10^{-6}
313	7.87×10^{-6}
318	9.26×10^{-6}
323	1.02×10^{-5}
328	1.20×10^{-5}
333	1.47×10^{-5}

Figure S14. Temperature dependence of Nyquist plots for the MOP-1 at 22% RH.

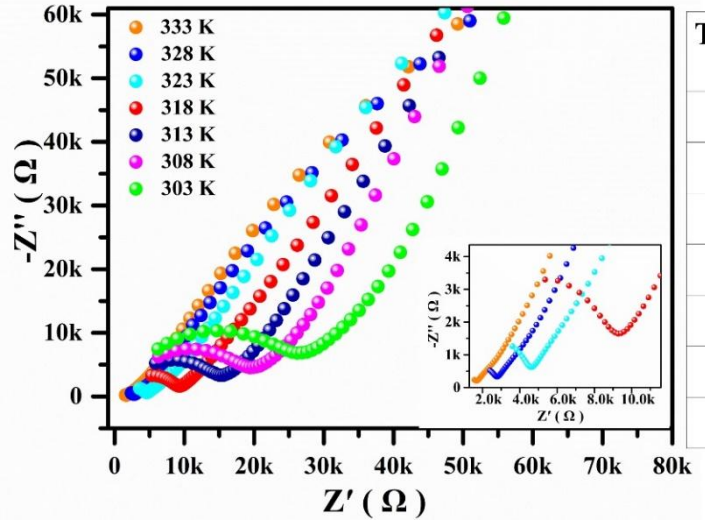

Temperature (k)	Conductivity (S cm^{-1})
303	1.94 × 10^{-5}
308	2.62 × 10^{-5}
313	3.32 × 10^{-5}
318	5.48 × 10^{-5}
323	1.10 × 10^{-4}
328	1.83 × 10^{-4}
333	3.02 × 10^{-4}

Figure S15. Temperature dependence of Nyquist plots for the MOP-1 at 53% RH.

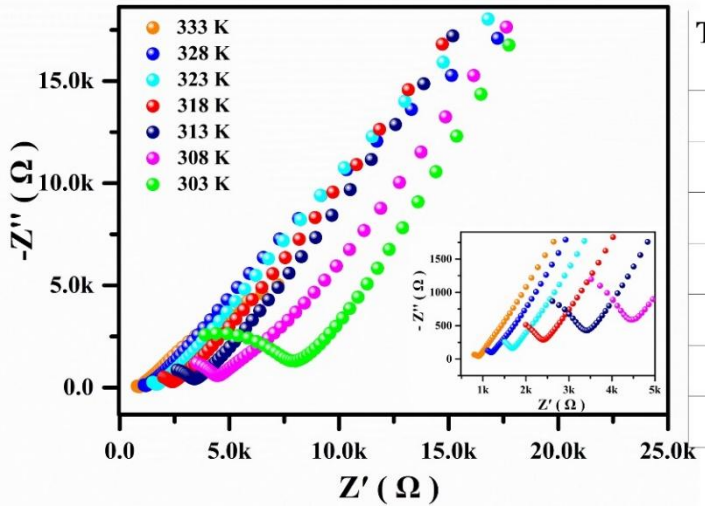

Temperature (k)	Conductivity (S cm^{-1})
303	6.54× 10^{-5}
308	1.14 × 10^{-4}
313	1.50 × 10^{-4}
318	2.11 × 10^{-4}
323	3.02 × 10^{-4}
328	4.26 × 10^{-4}
333	5.6 × 10^{-4}

Figure S16. Temperature dependence of Nyquist plots for the MOP-1 at 73% RH.

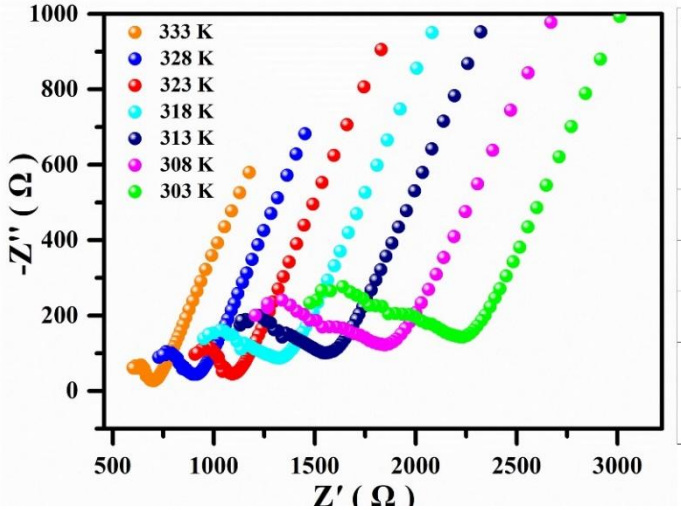

Temperature (k)	Conductivity (S cm^{-1})
303	2.28 × 10^{-4}
308	2.75 × 10^{-4}
313	3.26 × 10^{-4}
318	3.84 × 10^{-4}
323	4.64 × 10^{-4}
328	5.61 × 10^{-4}
333	7.25 × 10^{-4}

Figure S17. Temperature dependence of Nyquist plots for the MOP-1 at 93% RH.

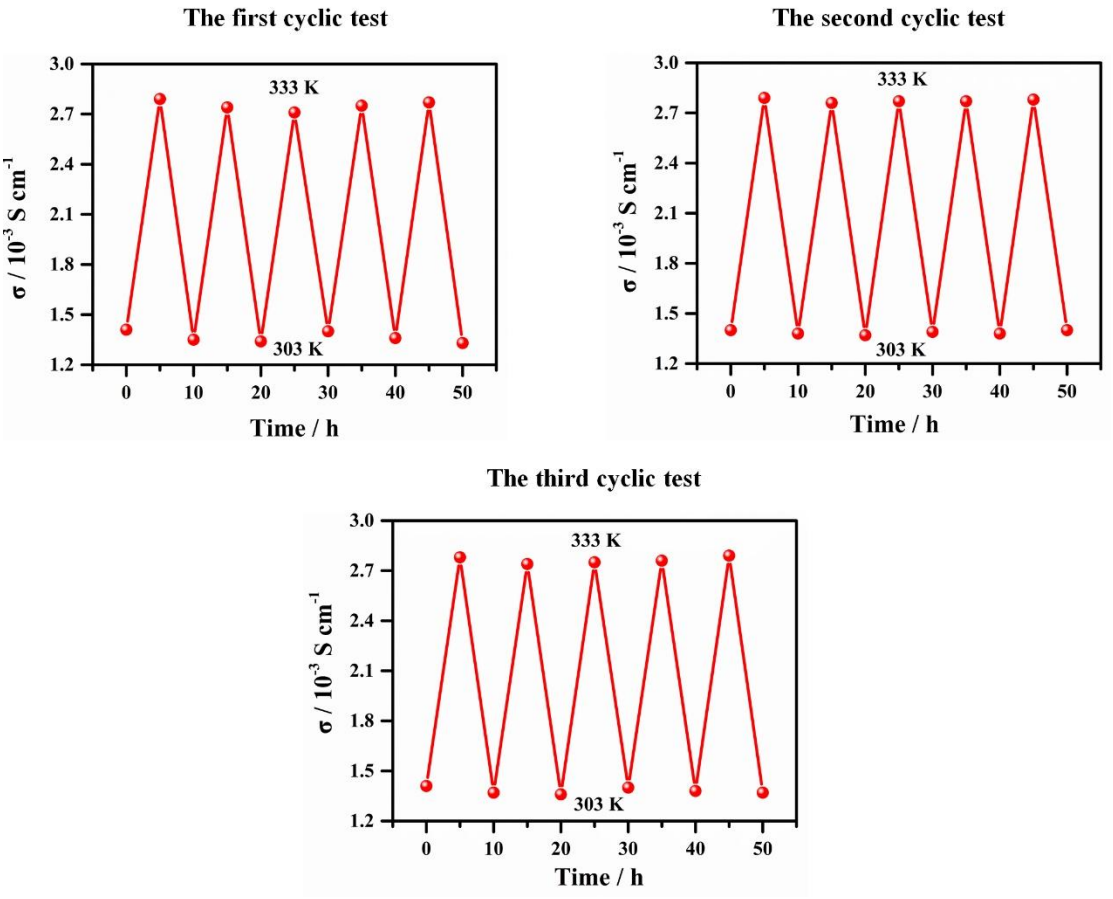

Figure S18. The cyclic stability test of proton conductivity.

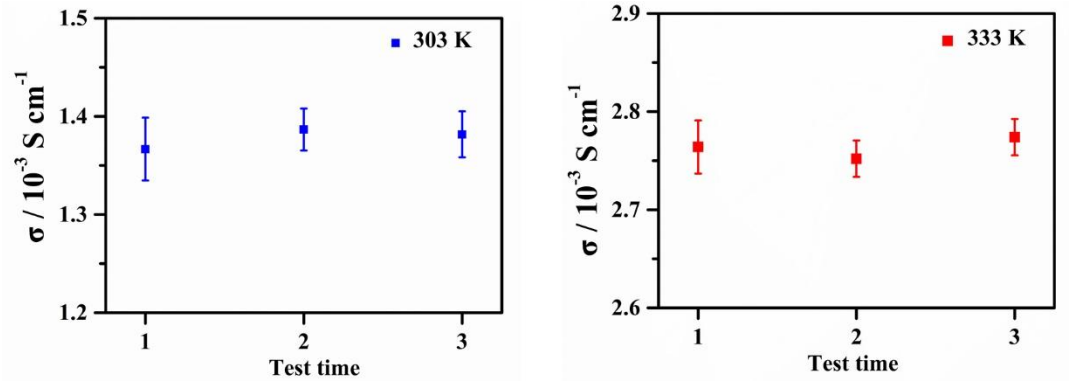

Figure S19. Error analysis of the three times cyclic stability test.

Table S1. Crystal data and structure refinement for cage-1.

Compound	MOP-1
Empirical formula	$C_{78}H_{73.92}Na_{3.96}O_{47.96}S_6Zr_6$
Formula weight	2609.37
Temperature/K	150
Crystal system	trigonal
Space group	R-3c
a/Å	16.2679(2)
b/Å	16.2679(2)

c/Å	84.1291(12)
α/°	90
β/°	90
γ/°	120
Volume/Å^3	19281.5(5)
Z	6
ρ_{calc}g/cm^3	1.348
μ/mm^{-1}	5.532
F(000)	7831.0
Crystal size/mm^3	0.15 × 0.15 × 0.1
Radiation	CuKα (λ = 1.54184)
2θ range for data collection/ °	10.498 to 134.946
Index ranges	-18 ≤ h ≤ 19, -14 ≤ k ≤ 19, -100 ≤ l ≤ 78
Reflections collected	17402
Independent reflections	3873 [R_{int} = 0.0317, R_{sigma} = 0.0289]
Data/restraints/parameters	3873/74/260
Goodness-of-fit on F^2	1.090
Final R indexes [I>=2σ (I)]	R_1 = 0.0480, wR_2 = 0.1464
Final R indexes [all data]	R_1 = 0.0512, wR_2 = 0.1490
Largest diff. peak/hole / e Å^{-3}	1.23/-0.93
CCDC number	1575660

$R_1 = \sum||F_o|-|F_c||/\sum|F_o|$. $wR_2 = [\sum w(F_o^2 - F_c^2)^2/\sum w(F_o^2)^2]^{1/2}$

Table S2. Selected bond lengths (Å) and bond angles (°) for MOP-1.

bond lengths (Å)			
Zr1−Zr1^1	3.3649(5)	Zr1−Zr1^2	3.3648(5)
Zr1−O1	2.0780(16)	Zr1−C2	2.524(4)
Zr1−O4^2	2.197(3)	Zr1−C3	2.548(4)
Zr1−O2^1	2.138(3)	Zr1−C4	2.527(4)
Zr1−O3	2.197(3)	Zr1−C5	2.509(5)
O1−Zr1^1	2.0779(16)	Zr1−C6	2.504(5)
O1−Zr1^2	2.0779(16)	O8−Na1A^3	2.592(9)
O4−Zr1^1	2.196(3)	O2−Zr1^2	2.138(3)
Na1A−S1^3	3.017(7)	Na1A−O10A	2.285(10)
Na1A−O7^3	2.414(6)	Na1A−O9B	2.49(3)
Na1A−O8^3	2.592(9)	Na1B−O10B	2.319(11)
S1−Na1A^3	3.016(7)	Na1B−O9A	2.294(10)
bond angles (°)			
Zr1^1−Zr1−Zr1^2	60.0	Zr1^1−O1−Zr1	108.12(12)
O1−Zr1−Zr1^2	35.94(6)	Zr1^2−O1−Zr1^1	108.12(12)
O1−Zr1−O4^1	78.69(12)	Zr1^2−O1−Zr1	108.12(12)
O1−Zr1−O2	73.31(11)	C10−S1−Na1A^3	113.0(2)
O1−Zr1−O3	79.87(11)	C7−O4−Zr1^2	128.2(3)
O1−Zr1−C2	152.64(12)	Zr1−O2−Zr1^1	103.78(12)

O1−Zr1−C3	151.80(14)	C7−O3−Zr1	127.6(3)
O1−Zr1−C6	152.53(16)	S1−O7−Na1A^{3}	99.3(2)
O1−Zr1−C4	151.38(15)	S1−O8−Na−1A	137.3(3)
O1−Zr1−C5	151.53(13)	S1−O8−Na1A^{3}	91.81(18)
O4^{1}−Zr1−Zr1^{1}	75.00(8)	S1−O8−Na1B	132.9(5)
O4^{1}−Zr1−Zr1^{2}	113.08(8)	Na1A−O8−Na1A^{3}	67.8(3)
O4^{1}−Zr1−C2	108.66(14)	C3−C2−Zr1	74.9(3)
O4^{1}−Zr1−C6	78.56(14)	C2−C3−Zr1	73.0(3)
O4^{1}−Zr1−C4	108.20(16)	C4−C3−Zr1	73.1(3)
O4^{1}−Zr1−C5	78.54(15)	C2−C6−Zr1	74.6(3)
O2^{2}−Zr1−Zr1^{2}	38.11(7)	C5−C6−Zr1	74.2(3)
O2−Zr1−Zr1^{2}	86.20(8)	C3−C4−Zr1	74.8(3)
O2^{2}−Zr1−Zr1^{1}	86.20(7)	C5−C4−Zr1	73.4(3)
O2−Zr1−Zr1^{1}	38.11(7)	C6−C5−Zr1	73.8(3)
O2−Zr1−O4^{1}	86.42(11)	C4−C5−Zr1	74.8(3)
O2^{2}−Zr1−O4^{1}	151.10(11)	O7^{3}−Na1A−S1^{3}	28.52(11)
O2−Zr1−O2^{2}	92.19(15)	O7^{3}−Na1A−O8^{3}	57.28(19)
O2^{2}−Zr1−O3	85.52(11)	O7^{3}−Na1A−Na1A^{3}	96.4(4)
O2−Zr1−O3	152.56(11)	O7^{3}−Na1A−O9B	96.5(4)
O2−Zr1−C2	132.26(13)	O8^{3}−Na1A−S1^{3}	28.99(10)
O2^{2}−Zr1−C2	93.54(14)	O8−Na1A−S1^{3}	123.9(3)
O2−Zr1−C3	104.11(14)	O8−Na1A−O7^{3}	152.4(4)
O2^{2}−Zr1−C3	78.80(13)	O8−Na1A−O8^{3}	95.2(3)
O2^{2}−Zr1−C6	125.76(15)	O8−Na1A−Na1A^{3}	62.4(2)
O2−Zr1−C6	120.21(15)	O8^{3}−Na1A−Na1A^{3}	49.8(2)
O2−Zr1−C4	79.34(13)	O8−Na1A−O10A	106.5(6)
O2^{2}−Zr1−C4	99.86(15)	O8−Na1A−O9B	103.2(5)
O2−Zr1−C5	88.43(15)	Na1A^{3}−Na1A−S1^{3}	74.0(3)
O2^{2}−Zr1−C5	130.31(15)	O10A−Na1A−S1^{3}	116.1(5)
O3−Zr1−Zr1^{1}	114.48(8)	O10A−Na1A−O7^{3}	94.8(5)
O3−Zr1−Zr1^{2}	75.18(8)	O10A−Na1A−O8^{3}	137.9(6)
O3−Zr1−O4^{1}	82.69(11)	O10A−Na1A−Na1A^{3}	168.7(6)
O3−Zr1−C2	75.17(13)	O10A−Na1A−O9B	83.4(9)
O3−Zr1−C3	102.25(14)	O9B−Na1A−S1^{3}	116.0(3)
O3−Zr1−C6	82.16(15)	O9B−Na1A−O8^{3}	126.7(6)
O3−Zr1−C4	128.01(13)	O9B−Na1A−Na1A^{3}	96.7(7)
O3−Zr1−C5	113.75(15)	O10B−Na1B−O8	135.4(13)
C2−Zr1−Zr1^{2}	124.17(12)	O9A−Na1B−O8	90.4(9)
C2−Zr1−Zr1^{1}	170.26(11)	O9A−Na1B−O10B	122.9(17)
C2−Zr1−C3	32.07(16)	O7−S1−Na1A^{3}	52.18(17)

C2−Zr1−C4	52.99(15)	O8−S1−Na1A^{3}	59.19(18)
C3−Zr1−Zr1^{2}	116.77(11)	C5−Zr1−Zr1^{2}	166.81(13)
C3−Zr1−Zr1^{1}	138.97(11)	C5−Zr1−Zr1^{1}	120.37(13)
C6−Zr1−Zr1^{2}	152.53(13)	C5−Zr1−C2	53.24(17)
C6−Zr1−Zr1^{1}	146.19(13)	C5Zr1C3	53.16(16)
C6−Zr1−C2	32.28(17)	C5−Zr1−C4	31.78(18)
C6−Zr1−C3	53.19(16)	C4−Zr1−Zr1^{1}	117.45(11)
C6−Zr1−C4	52.78(18)	C4−Zr1−Zr1^{2}	135.08(14)
C6−Zr1−C5	32.02(18)	C4−Zr1−C3	32.12(16)

Symmetry codes: ^{1}1+Y-X, 1-X, +Z;^{2} 1-Y, +X-Y, +Z;^{3} 4/3-X, 2/3-X+Y, 7/6-Z;^{4} 1/3+Y, -1/3+X, 7/6-Z

Supporting references:

1 G. Liu, Z. Ju, D. Yuan, M. Hong, *Inorg. Chem.* 2013, **52**, 13815

2 A. L. Myers and J. M. Prausnitz, *AIChE J.*, 1965, **11**, 121.

3 Q.-H. Yue, X.-H. Shao and D.-P. Cao, *Acta Physico-Chimi Sinica*, 2007, **23**, 1080.